Controlling the Phase-Space Volume of Injected Electrons in a Laser-Plasma Accelerator

C. Rechatin,[1] J. Faure,[1] A. Ben-Ismail,[1,2] J. Lim,[1] R. Fitour,[1] A. Specka,[2] H. Videau,[2] A. Tafzi,[1] F. Burgy,[1] and V. Malka[1]

[1]*Laboratoire d'Optique Appliquée, ENSTA, CNRS, École Polytechnique, UMR 7639, 91761 Palaiseau, France*
[2]*Laboratoire Leprince Ringuet, École Polytechnique, CNRS-IN2P3, UMR 7638, 91128 Palaiseau, France*

To take full advantage of a laser-plasma accelerator, stability and control of the electron beam parameters have to be achieved. The external injection scheme with two colliding laser pulses is a way to stabilize the injection of electrons into the plasma wave, and to easily tune the energy of the output beam by changing the longitudinal position of the injection. In this Letter, it is shown that by tuning the optical injection parameters, one is able to control the phase-space volume of the injected particles, and thus the charge and the energy spread of the beam. With this method, the production of a laser accelerated electron beam of 10 pC at the 200 MeV level with a 1% relative energy spread at full width half maximum (3.1% rms) is demonstrated. This unique tunability extends the capability of laser-plasma accelerators and their applications.

Laser wakefield accelerators hold the promise of compact electron beam sources [1]. In such an accelerator, electrons are trapped and accelerated in a longitudinal plasma wave whose velocity v_p is close to the speed of light c. In electric fields of several hundreds of GV/m, electrons can reach ultrarelativistic energies on a millimeter scale. This alternative acceleration technique has made remarkable progress over the last few years. In 2004, it was first proven that under certain laser and plasma conditions the "bubble regime" could lead to the production of quasimonoenergetic electron beams [2–4]. In this regime, an almost spherical ionic cavity of size corresponding to the plasma wavelength λ_p is formed behind the laser pulse [5,6]. A spike in the electron density builds up at the back of the cavity and eventually breaks, causing electron injection. Because they are localized in space and time, those electrons witness the same accelerating field and are accelerated with small energy spread. At the time of those first experiments, stability and control of the beam parameters were not addressed, the whole process being highly nonlinear. Recent improvements of this scheme have led to a more stable beam, either using capillaries [7,8] or gas jets [9,10]. An alternative approach using two colliding laser pulses marked a significant improvement in the electron beam stability and control of energy. It relies on an optical injection scheme in which a second laser pulse (injection pulse) imparts a momentum kick to electrons so that they can remain in the accelerating phase of the plasma wave. This basic idea, first developed in [11], was refined to a scheme in which the initial momentum is given by the ponderomotive beat wave of the two lasers when they collide [12,13]. This injection mechanism does not rely on nonlinear effects and therefore allows for the injection of electrons in a stable manner [14,15]. Moreover, by decoupling the injection and acceleration processes, it is possible to gain control over electron beam parameters

without changing the laser driving the plasma wave (pump pulse) or the plasma parameters. By changing the collision position and therefore the acceleration length, it has been already proven in [14] that the energy of the beam can be controlled. In this Letter, we show that we can also use the injection pulse amplitude and polarization to control the phase-space volume of the injected electrons, and hence the charge and energy spread of the accelerated electron beam. This demonstrates control over the relevant parameters of the laser-plasma accelerator.

We report here the results of an experiment conducted with the Laboratoire d'Optique Appliquée "Salle Jaune" Ti:Sa laser system, which delivers two ultrashort 30 fs linearly polarized pulses. The pump pulse is focused to intensities up to $I_0 = 4.6 \times 10^{18}$ W · cm^{-2}, which corresponds to a normalized amplitude of $a_0 = 1.5$. The injection pulse is focused with intensities up to $I_1 = 4 \times 10^{17}$ W · cm^{-2}, for which $a_1 = 0.4$. A supersonic helium gas jet, after ionization by the front of the laser pulses, provides the plasma medium. In this experiment two different gas jets have been used and characterized independently by interferometry. A 2 mm nozzle, which has a slightly parabolic density profile, with a plateau over only 0.8 mm and a 3 mm nozzle with a well defined density plateau over 2.1 mm. The differences in length and profile of the two gas jets lead to two different electron densities of operation: typically 1.2×10^{19} cm^{-3} for the 2 mm nozzle and 5.7×10^{18} cm^{-3} for the 3 mm nozzle. The two laser beams propagated with a 176° angle, instead of 180° as in previous colliding pulse experiments [14,15]. This noncollinear geometry offers several advantages: (i) it minimizes the risk of damaging the laser system by reducing the laser feedback to less than 1 mJ; (ii) the electron beam can be extracted and diagnosed more easily because there are no optics in its path. The electron beam is measured with a spectrometer consisting of a dipole mag-

net (1.1 T over 10 cm) and a LANEX phosphor screen. It gives access to energy distribution, charge, and angular distribution of the electron beam [16]. A half-wave plate followed by a polarizer enables us to reduce the injection pulse energy before compression. A second half-wave plate enables us to rotate the polarization of the injection pulse.

External injection provides a way to dramatically stabilize the injection process and the production of a quasimonoenergetic beam. A data set of 30 consecutive shots taken with the 3 mm nozzle, density $n_e = 5.7 \times 10^{18}$ cm^{-3} and collision position $z_{coll} = -400$ μm (the z axis is oriented in the direction of the pump pulse with origin in the center of the gas jet), yields a very stable beam in energy $E = 206 \pm 10$ MeV (5% rms fluctuation) with measured full width at half maximum (FWHM) energy spread $\Delta E = 14 \pm 3$ MeV (20% rms fluctuation) (limited by the resolution of the spectrometer), FWHM divergence $\theta = 4.5 \pm 1.6$ mrad (36% rms fluctuation), and peak charge $Q_{pk} = 13 \pm 4$ pC (30% rms fluctuation). For this data set the laser energy fluctuation is 17% rms and 60% peak to peak. We have also witnessed that fluctuations of the electron beam parameters depend on laser stability. The reproducibility of a high quality beam is the first feature required by numerous applications of an electron source. This is also crucial for accurate measurements of beam parameters such as bunch duration or emittance measurements which often require a complete set of reproducible data.

Finally, it also enables us to see statistically clear variations of the beam parameters over a low number of shots (typically 3–5), thus justifying the following parametric study.

By changing the delay between the pump and injection pulses, one is able to change the longitudinal position of injection. Therefore, it is possible to control the acceleration length and, consequently, the energy of the output electron beam. It was already proven in a collinear geometry and still holds with a large colliding angle $\alpha = 176°$ since the pulses collide over a spatial region longer than 1 mm. Using the 3 mm gas jet with $n_e = 5.7 \times 10^{18}$ cm^{-3}, we were able to tune the final energy continuously from 60 to 230 MeV.

In addition to the collision position, the use of an external injection scheme makes it possible to change the parameters of the injected electron beam without modifying the accelerating structure induced by the pump pulse and its coupling to the plasma. Control over the injection pulse parameters, namely, intensity and polarization, translates into control over the injection process and enables us to modify the phase-space volume of the injected particles. A simplistic physical picture for a one-dimensional (1D) case with circularly polarized laser pulses is represented in Fig. 1. Assuming $a_0 = 2$, $n_e = 7 \times 10^{18}$ cm^{-3}, and a Gaussian pulse of 30 fs duration, one can compute the 1D separatrix for the wakefield, which is
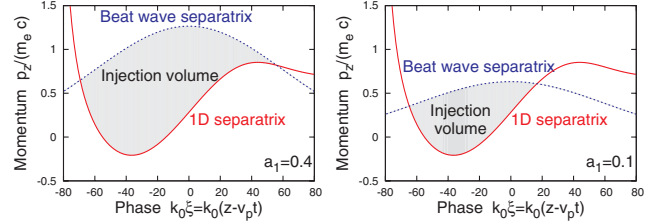
FIG. 1 (color online).   Evolution of injection volume with a_1 for $a_0 = 2$, $n_e = 7 \times 10^{18}$ cm^{-3}. Left: $a_1 = 0.4$. Right: $a_1 = 0.1$. Fields are computed for the 1D case, and the beat wave separatrix corresponds to the circular polarization case.

the boundary, in longitudinal phase space, between trapped particles and untrapped particles (red solid curve). For circularly polarized lasers, since the motion is deterministic, one can also compute the beat wave separatrix which gives the maximum momentum gain that can be achieved in the beat wave (blue dotted curve). Following the approach of [13], i.e., using a Chirikov criterion, injection will occur when the two separatrices overlap, thus defining an injection volume in phase space. Here, a decrease of a_1 lowers the beat wave separatrix and reduces directly the injection volume. The reality is more complex since heating with linearly polarized lasers is stochastic [17,18] and we also know that the underlying fluid approximation used for describing the wake potential does not hold at the collision position. The electrons are indeed trapped in the beat wave and cannot take part in the large scale oscillations driving the plasma wave. As a consequence, the wakefield is less suitable for trapping and the injection phase-space volume is reduced compared to the above idealized case [19]. However, stochastic heating with linearly polarized lasers is a growing function of a_1, and the injection is still a threshold process. Therefore, the simplistic picture still holds, and the injection volume can be made arbitrarily small by changing the injection parameters.

Experimentally, changing the energy gain of electrons during the collision can be performed in two different ways: (i) by changing the injection pulse energy (with a half-wave plate and polarizer placed before the grating compressor) since the longitudinal momentum gain of electrons in the beat wave scales as $\sqrt{a_0 a_1}$ and (ii) by using the polarization dependence of the beat wave mechanism. The heating of the electrons is indeed more effective when the polarizations of the pulses are parallel. When the polarizations are crossed, heating is less efficient but injection can still occur [20].

Evidently, tuning the injection volume results in the control of the charge injected in the main accelerating structure. Figure 2 (top) shows raw electron spectra obtained with the 2 mm gas nozzle and an electron density of $n_e = 1.2 \times 10^{19}$ cm^{-3} for different injection laser amplitudes. It confirms that the charge, corresponding to the
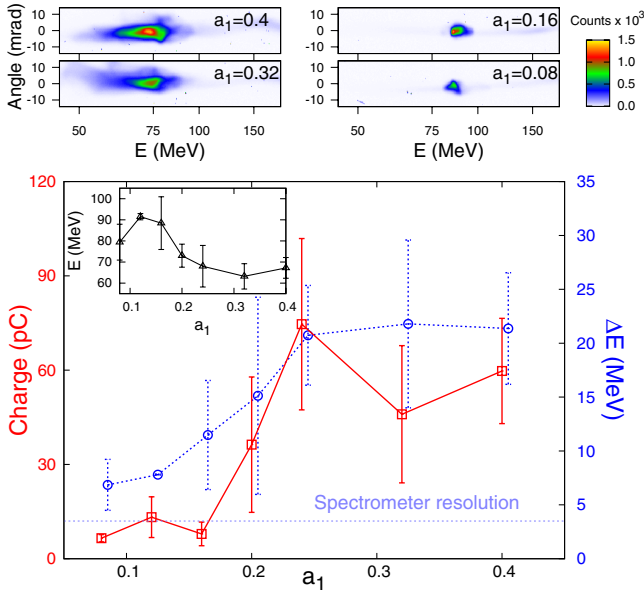
FIG. 2 (color online). Top: Raw electron spectra for different a_1. The horizontal axis is the dispersive direction so that the abscissa represents the energy of the beam (nonlinear scale). The nondispersive direction gives information on the divergence of the beam. Bottom: Evolution of charge (red solid line with squares), ΔE at FWHM (blue dotted line with circles) with a_1. The error bars represent the rms fluctuation. Inset : variation of peak energy. Physical parameters: $a_0 = 1.4$, 2 mm gas jet, $n_e = 1.2 \times 10^{19}$ cm^{-3}, $z_{coll} = -100$ μm.

integral of the number of counts, can be tuned for beam energies in the 70–80 MeV range.

The parameters of the electron beams for the data set are summarized in Fig. 2 (bottom). The solid (red) line represents the evolution of the charge in the monoenergetic component with the injection pulse amplitude. It shows that injection of electrons was obtained for normalized injection pulse amplitudes as low as $a_1 = 0.1$, giving a 6 pC electron beam. The charge then rapidly increases for low injection amplitudes and then saturates at 60 pC for normalized injection amplitudes ranging from 0.25 to 0.4. This behavior is consistent with 1D PIC simulations [20] and can be explained as follows: on one hand the momentum gain increases with the injection pulse intensity, but on the other hand the wakefield inhibition [19] also becomes stronger with the injection pulse intensity. This process makes trapping harder and eventually balances the injected charge. Simulations also show that for higher values of injection laser amplitude $a_1 > 1$, the charge becomes again a growing function of a_1, when the wake is completely inhibited.

The control of the charge can also be achieved by rotating the injection pulse polarization. Figure 3 shows a data set taken with the 3 mm gas nozzle and an electron density of $n_e = 5.7 \times 10^{18}$ cm^{-3}. The red curve represents the injected charge evolution with the angle between the polarizations of the two pulses. As expected, the charge is
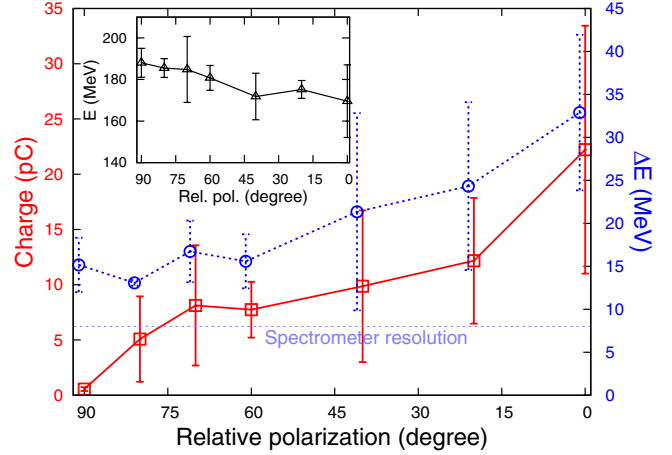
FIG. 3 (color online). Evolution of charge (red solid line with squares), ΔE at FWHM (blue dotted line with circles) with the angle between the polarizations of injection and pump lasers (0°, parallel polarizations; 90°, crossed polarizations). Inset : variation of peak energy. Physical parameters: $a_0 = 1.5$, $a_1 = 0.4$, 3 mm gas jet, $n_e = 5.7 \times 10^{18}$ cm^{-3}, $z_{coll} = -450$ μm.

maximal (22 pC) when the injection pulse has the same polarization as the pump pulse (0° angle) and decreases to its minimal value (1 pC) when the polarizations are crossed (90° angle). Here, the beam peak energy is about 180 MeV, showing that tuning the charge can be performed at various energy levels.

The insets in Figs. 2 and 3 show that the peak energy slightly drops as the injected charge increases : from 90 to 70 MeV for Fig. 2 and from 190 to 170 MeV for Fig. 3. This decrease can be explained by the combination of two effects: (i) injection in lower energy gain orbits, further from the separatrix; (ii) beam loading effects [21]. The full explanation of this interplay is beyond the scope of this Letter and is the topic of another paper [22]. Nevertheless, this small variation can be easily compensated by adjusting the collision position and by adding about 100 μm to the acceleration length.

Furthermore, the change of injection volume also impacts the energy spread of the beam. Indeed, in the small charge limit, when beam loading effects are negligible, the acceleration process can be described by Hamiltonian theory in which the quantity $\Delta p \Delta x$ is conserved during the acceleration: a small injection volume will result in small energy spread after acceleration. On the contrary, larger injection volumes will result in larger energy spreads. In addition, when the injection volume (and hence the charge) grows, beam loading effects become more important and will also tend, if uncontrolled, to produce greater energy spread after acceleration [21]. When a high charge is accelerated, it indeed distorts the wakefield and can broaden the energy spectrum of the beam. Beam loading effects in this experiment are specifically addressed in another paper [22].
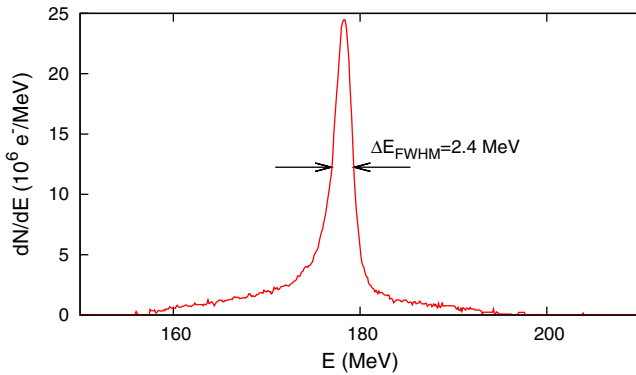
FIG. 4 (color online).   Deconvoluted spectrum from high reso-
lution spectrometer measurement. Physical parameters: $a_0 =$
1.2, $a_1 = 0.35$, 3 mm gas jet, $n_e = 7.1 \times 10^{18}$ cm^{-3}, $z_{coll} =$
-300 μm.

In all cases, increasing the injection volume will increase
the energy spread, either directly or indirectly through
beam loading effects. That is why charge and energy
spread are strongly correlated, as can be seen in Figs. 2
and 3, also representing the FWHM width of the quasi-
monoenergetic peak ΔE (blue circles). In Fig. 2, the energy
spread can be tuned from 22 to 7 MeV, and in Fig. 3, the
energy spread is reduced from 33 to 13 MeV. For both data
sets, the linear correlation factor between charge and spec-
tral width ΔE is 0.8.

This evolution of the energy spread has important im-
plications since the narrower energy distribution almost
compensates the charge decrease, so that the spectral in-
tensity and brilliance of the electron beam stays nearly the
same (within a factor of 2). If extrapolated, this technique
can lead to even narrower energy distributions, as heating
can be tuned as close to the injection threshold as neces-
sary. Both Figs. 2 and 3 show that the measurement of the
energy spread is limited by the spectrometer resolution.
Thus, in order to resolve the electron spectrum, we used a
focusing-imaging spectrometer whose resolution is better
than 1%.

Figure 4 shows a measurement performed using this
spectrometer. The parameters were 3 mm gas nozzle, $n_e =$
7.2×10^{18} cm^{-3}, and the laser intensities were slightly
lower, $a_0 = 1.2$ and $a_1 = 0.35$. The electron spectrum
exhibits a very narrow energy distribution with a monoen-
ergetic peak at 178 MeV of width 2.4 MeV FWHM, giving
a relative energy spread (FWHM) of 1.3%. Note that the
whole charge of the beam (11 pC) is contained in this
narrow peak, yielding a total rms energy spread of only
3.1%. The divergence of this beam is 3 ± 1 mrad, which
leads to an estimated resolution for this shot of ‰.

This scheme therefore holds the promise of producing
very narrow energy distributions not only suitable for all
applications demanding high temporal resolution but also
for free electron laser experiments that are strongly depen-
dent on beam quality, and, in particular, energy spread.

In this Letter, we have demonstrated that the use of
optical external injection not only enables us to stabilize
and control the energy of the electron beam but also
provides "knobs" to easily change the injection volume,
thus allowing the modification of the charge along with the
energy spread. This method provides a way to improve
beam quality, and energy spreads of 1.3% FWHM have
been measured. This high quality, stable, and fully tunable
beam produced by a laser-plasma accelerator paves the
way for numerous applications.

[1] T. Tajima and J. M. Dawson, Phys. Rev. Lett. **43**, 267
     (1979).
[2] S. P. D. Mangles *et al.*, Nature (London) **431**, 535 (2004).
[3] C. G. R. Geddes *et al.*, Nature (London) **431**, 538 (2004).
[4] J. Faure *et al.*, Nature (London) **431**, 541 (2004).
[5] A. Pukhov and J. Meyer-ter-Vehn, Appl. Phys. B **74**, 355
     (2002).
[6] W. Lu *et al.*, Phys. Rev. Lett. **96**, 165002 (2006).
[7] W. P. Leemans *et al.*, Nature Phys. **2**, 696 (2006).
[8] J. Osterhoff *et al.*, Phys. Rev. Lett. **101**, 085002 (2008).
[9] S. P. D. Mangles *et al.*, Phys. Plasmas **14**, 056702
     (2007).
[10] N. A. M. Hafz *et al.*, Nat. Photon. **2**, 571 (2008).
[11] D. Umstadter, J. K. Kim, and E. Dodd, Phys. Rev. Lett. **76**,
     2073 (1996).
[12] E. Esarey *et al.*, Phys. Rev. Lett. **79**, 2682 (1997).
[13] G. Fubiani, E. Esarey, C. B. Schroeder, and W. P. Leemans,
     Phys. Rev. E **70**, 016402 (2004).
[14] J. Faure *et al.*, Nature (London) **444**, 737 (2006).
[15] J. Faure *et al.*, Plasma Phys. Controlled Fusion **49**, B395
     (2007).
[16] Y. Glinec *et al.*, Rev. Sci. Instrum. **77**, 103 301 (2006).
[17] Z.-M. Sheng *et al.*, Phys. Rev. Lett. **88**, 055004 (2002).
[18] J. T. Mendonça, Phys. Rev. A **28**, 3592 (1983).
[19] C. Rechatin *et al.*, Phys. Plasmas **14**, 060 702 (2007).
[20] C. Rechatin *et al.*, New J. Phys. **11**, 013 011 (2009).
[21] T. Katsouleas *et al.*, Part. Accel. **22**, 81 (1987).
[22] C. Rechatin *et al.* (unpublished).